Biochemical and Biophysical Research Communications 457 (2015) 31–36

Contents lists available at ScienceDirect

Biochemical and Biophysical Research Communications

journal homepage: www.elsevier.com/locate/ybbrc

Silk gland-specific proteinase inhibitor serpin16 from the *Bombyx mori* shows cysteine proteinase inhibitory activity

Peng-Chao Guo, Zhaoming Dong, Li Xiao, Tao Li, Yan Zhang, Huawei He, Qingyou Xia, Ping Zhao *

State Key Laboratory of Silkworm Genome Biology, Southwest University, 216, Tiansheng Road, Beibei, Chongqing 400716, People's Republic of China

ARTICLE INFO

Article history:
Received 2 December 2014
Available online 18 December 2014

Keywords:
Serpin (**ser**ine **p**roteinase **in**hibitor)
Bombyx mori
Silk gland-specific
Inhibitory activity
Structure

ABSTRACT

Serpins (**ser**ine **p**roteinase **in**hibitor**s**) are widely distributed in different species and are well known for their inhibitory activities towards serine proteinases. Here, we report the functional characterization of *Bombyx mori* serpin16. Expression analysis showed that serpin16 was specifically expressed at high levels in the silk gland at both the transcriptional and translational levels. Moreover, homology modeling and multi-sequence alignment suggested that serpin16 had a canonical serpin fold, but it contained a unique reactive center loop, which was obviously shorter than that of typical serpins. Inhibitory activity analyses revealed that the target proteinase of serpin18 is a cysteine proteinase, rather than a serine proteinase. Furthermore, a Michaelis complex model of serpin16 with its target proteinase was constructed to explain the structural basis of how serpin16 recognizes the cysteine proteinase and its target specificity.

1. Introduction

Serpins (**Ser**ine **p**roteinase **in**hibitor**s**) are a ubiquitous family of proteins with diverse functions [1], including blood coagulation, fibrinolysis, embryonic development, and programmed cell death [2–4]. A recent authoritative classification of known peptide inhibitors showed that serpins are commonly distributed in all three super-kingdoms of life—eukarya, bacteria and archaea—as well as in certain viruses [5]. Most serpins are found in multicellular eukaryotes and inhibit serine proteases, while some members of the super-family can either inhibit cysteine proteinases, such as the antithrombin [6,7], or lack any proteinase inhibitory property, such as ovalbumin [8], angiotensinogen [9], and thyroxine binding globulin [10,11]. Typical serpins share about 30% sequence homology as well as a common fold composed of three β-sheets and nine α-helices, and a reactive center loop (RCL) [12]. In the inhibition reaction, serpins employ the RCL to bait target serine proteases and form a Michaelis complex, which is the critical step in the ultimate trapping of a proteinase. Then, the RCL inserts into β-sheet A of the serpin protein, carrying the covalently bound proteinase from the top to bottom of the serpin [3].

In recent decades, serpins have been identified from many insects, including *Bombyx mori* [13], *Manduca sexta* [14], *Mythimna unipuncta* [15], and *Aedes aegypti* [16]. In *B. mori*, 34 serpin genes have been identified and their reactive sites were predicted [17]. Among these serpins, only a few have been studied. Initially, two serpins, antichymotrypsin and antitrypsin, were identified in the hemolymph of *B. mori* [18,19]. In the 1990's, an additional antichymotrypsin was cloned from the larval fat body and termed antichymotrypsin II [20]. Recently, two serpin-type inhibitors, Bmb041993 and Bmb015591, were identified in the silk gland using two-dimensional electrophoresis and mass spectrometry [21]. We found that these two serpins corresponded to serpin16 and serpin18 proteins, which are two of the 34 serpins of *B. mori* reported by Zou et al. [17]. These two genes are highly similar and syntenic and show 92% cDNAs identity. Serpin18 (with Ala at the P1 position) was predicted to control elastase-like enzymes, whereas the target enzymes of serpin16 have remained uncertain, since a Glu residue is located at the P1 position [17]. To functionally characterize the serpin16 and understand its physiological roles, we expressed the recombinant serpin16 and detected its activity. Expression profile and inhibitory activity analysis revealed that serpin16 acts as a cysteine proteinase inhibitor that can regulate protease activities in the silk gland of silkworms. Moreover, a homology model of serpin16 and a docking model with its target proteinase were constructed to explain the mechanism underlying serpin16 target specificity.

2. Materials and methods

2.1. Sample preparation and expression analysis of serpin16

The silkworm strain DAZAO, maintained in the State Key Laboratory of Silkworm Genome Biology (Southwest University,

* Corresponding author. Fax: +86 23 68250099.
E-mail address: zhaop@swu.edu.cn (P. Zhao).

http://dx.doi.org/10.1016/j.bbrc.2014.12.056
0006-291X/

China), was bred routinely on mulberry leaves at 25 ± 1 °C with 70 ± 5% humidity. Silk glands, ovaries, fat bodies, midguts, integuments, hemocytes, Malpighian tubules, heads, maxillary palpus, and antennae from day 3 of fifth instar larvae were dissected on ice. All tissues were immediately frozen in liquid nitrogen and stored at −80 °C for RNA isolation or protein extraction.

2.2. Cloning and expression of wild-type and mutant serpin16

The open reading frame of *SERPIN16* was amplified by PCR, using *B. mori* (strain p50, Dazao) silk gland cDNA as the template. The PCR product was inserted into a pET28a-derived vector and transformed into the *Escherichia coli* BL21 (DE3) strain. The serpin16-expressing cells were induced with 0.2 mM isopropyl-β-D-thiogalactoside at 37 °C for 4 h when $OD_{600\ nm}$ reached 0.6. Cells were harvested by centrifugation at 6000×*g* for 10 min and then were resuspended in lysis buffer (20 mM Tris–HCl, pH 6.8, 200 mM NaCl). After 5 min of sonication and centrifugation at 12,000×*g* for 25 min, supernatants were collected and loaded onto a HiTrap nickel-chelating column (GE Healthcare) equilibrated with binding buffer (20 mM Tris–HCl, pH 6.8, 200 mM NaCl). The target protein was eluted with 250 mM imidazole buffer and then was loaded onto a HiLoad 16/60 Superdex 200 column (GE Healthcare) equilibrated with 20 mM Tris–HCl, pH 6.0, 50 mM NaCl. The purity of the eluted protein was estimated by SDS–PAGE and the protein sample was stored at −80 °C. The mutant proteins were expressed, purified, and stored in the same manner as the wild-type protein.

2.3. Computational modeling and docking

A structural model of serpin16 was constructed based on the crystal structure of serpin18 from *B. mori* (PDB: 4R9I) using SWISS-MODEL [22–24]. Docking runs were performed using the program HADDOCK [25] based on our serpin16 model and the structure of papain (PDB: 1PPP). Up to 15 initial clusters were generated, and for each multiple conformations were scored. The pose with the best score was rigid-body minimized and then assessed for electrostatic and van der Waals interactions.

2.4. Inhibitory activity assay

To assay papain inhibition, 20 μg papain was mixed in a 1.5 ml tube with varying amounts of wild-type or mutant serpin16 to a final volume of 100 μl. After incubation for 30 min at room temperature, 400 μl azocasein (Sigma) in 20 mM $NaHCO_3$, pH 8.1 was added to the reactions at 37 °C for 30 min. The reaction was terminated by adding 1 ml 10% (w/v) trichloroacetic acid solution. The assay mixture was centrifuged at 13,000×*g* for 10 min, then an equal volume of 1.0 M NaOH was added to the supernatant and absorbance was measured at 440 nm using a DU800 spectrophotometer (Beckman Coulter).

3. Results and discussion

3.1. Serpin16 sequence analysis and its expression profile

The putative *Serpin16* cDNA encoded a 392 amino acid protein with a 20 amino acid residue signal peptide (Fig. 1A), indicating that serpin16 might be secreted into the extracellular milieu. After removal of the signal peptide, the matured protein was predicted by analysis with the Expasy server to be 43 kDa with a theoretical pI of 4.6. BLAST analysis of the putative conserved domain showed that matured serpin16 was composed of a relative conserved serpin family domain and a non-conserved N-terminal region

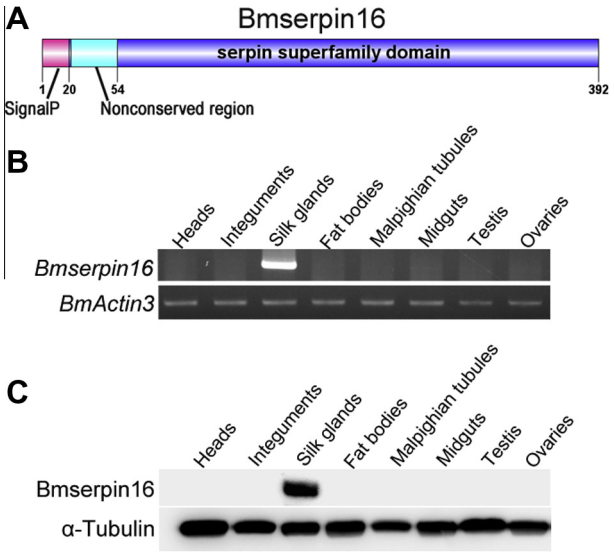

Fig. 1. Expression patterns of serpin16 in the silkworm. (A) A diagram to show the organization of serpin16. (B) Expression patterns of *serpin16* genes in various tissues from day 3 of the fifth instar. The silkworm cytoplasmic actin A3 gene (*Bmactin3*; GenBank Accession No. U49854) was used as internal control. (C) Western blot analysis for serpin16 in the different tissues from day 3 of the fifth instar.

(Fig. 1A). We expressed serpin16 in *E. coli* BL21 (DE3) in a soluble form and purified it to homogeneity; the purity was confirmed using SDS–PAGE. Gel filtration analysis indicated that serpin16 eluted at a volume corresponding to ~80 kDa (Fig. S1A), which is approximately double its theoretical molecular weight of 43 kDa (Fig. S1B). Thus, these findings indicated that serpin16 exists as a dimer in solution.

The expression of serpin16 in different tissues was analyzed by reverse transcription-PCR (RT-PCR). Tissues were dissected out from larvae on day 3 of fifth instar larvae. Signals were only detected in the silk gland, and no signal was observed in the other tissues. These results showed that *Bmserpin16* is highly and specifically expressed in silk glands (Fig. 1B). To confirm its expressional specificity in the silk gland at the protein level, a polyclonal antibody against serpin16 was produced to analyze the different tissues in day 3 of the fifth instar larvae. Western blots showed that serpin16 was only expressed in the silk gland, which was consistent with our semi-quantitative RT-PCR analyses (Fig. 1C). Furthermore, immunofluorescence analysis showed that serpin16 signals could be observed in the lumen of the silk gland and in the gland cells (unpublished data), suggesting that serpin16 was secreted from silk gland cells into the lumen.

3.2. Structural characterization of serpin16

Preliminary crystallographic analyses showed that stick-like crystals appeared in a drop consisting of 5% (v/v) Tacsimate pH 7.0, 0.1 M HEPES, pH 7.0 and 10% PEG 5000MME (Fig. S1C). Diffraction data were collected from a single crystal to 3.0 Å resolution. The crystal belongs to space group $P6_422$, with unit-cell parameters a = 73.426, b = 73.426, and c = 107.428. However, the quality of the diffraction data was not ideal, and further refinement of the crystal and associated structure is ongoing.

A homology structure of serpin16 was obtained via SWISS-MODEL using the known structure of serpin18 from silkworm (PDB: 4R9I, unpublished data) as a temple. The sequence identity between the temple and serpin16 was 87.1% and the QMEAN Z-Score was −1.15 for the serpin16 model. The root-mean-square

deviation (RMSD) between the model and 4R9I was 0.03 Å. The overall structure of the homology model is shown in Fig. 2A. The protein adopts a classical serpin fold, which includes three β-sheets (βA, βB, and βC), nine helices, and a reactive center loop that is exposed to solvent. Superposition of serpin16 against the typical serpin *Hs*PAI-1 (*Homo sapiens* plasminogen activator inhibitor-1) structure yielded an overall RMSD of 5.1 Å over approximately 271 Cα atoms, implying that there are several structural features of serpin16 that are different from the structure of typical serpin (Fig. 2B). In a higher resolution analysis of the structure, we found that the helices adopt a similar pattern to other serpins. The major differences between serpin16 and *Hs*PAI-1 are in the RCL regions and surrounding β-strands. Notably, the RCL of serpin16 is closer to β-sheet C of the protein in comparison to that of the classical serpin. Meanwhile, the β-sheet C bent more towards the core of the protein in comparison to that of the classical serpins, creating more room for the RCL. The counterpart of a short helix near the RCL in typical serpin is relaxed into a β-strand (designed β1C) in serpin16 and is bent towards the core of the molecule, leaving space for RCL (Fig. 2B). Additionally, the top of β-sheet A from serpin16 shifts to the helix hD and forms a more compact conformation compared to that of *Hs*PAI-1 (Fig. 2B). Furthermore, multiple-sequence alignment and structural analyses showed that the length of the RCL in serpin16 is shorter by approximately seven amino acids than that of typical serpins (Fig. 2C). The RCL of typical serpins is composed of approximately 24 amino acids, whereas the RCL of serpin16 is only 17 amino acids in length. Previous studies suggested that the residue composition and length of the RCL are directly related to the proteinase specificity [26] and inhibitory mechanism in typical serpins [27]. Thus, these differences in the RCL between serpin16 and its counterparts imply that serpin16 might possess distinct target specificity and inhibitory mechanism.

3.3. Inhibitory activities of serpin16

To evaluate the inhibitory activity of serpin16, we tested its activities in an inhibition reaction using commercial proteinases as targets, including five serine proteinases and two cysteine

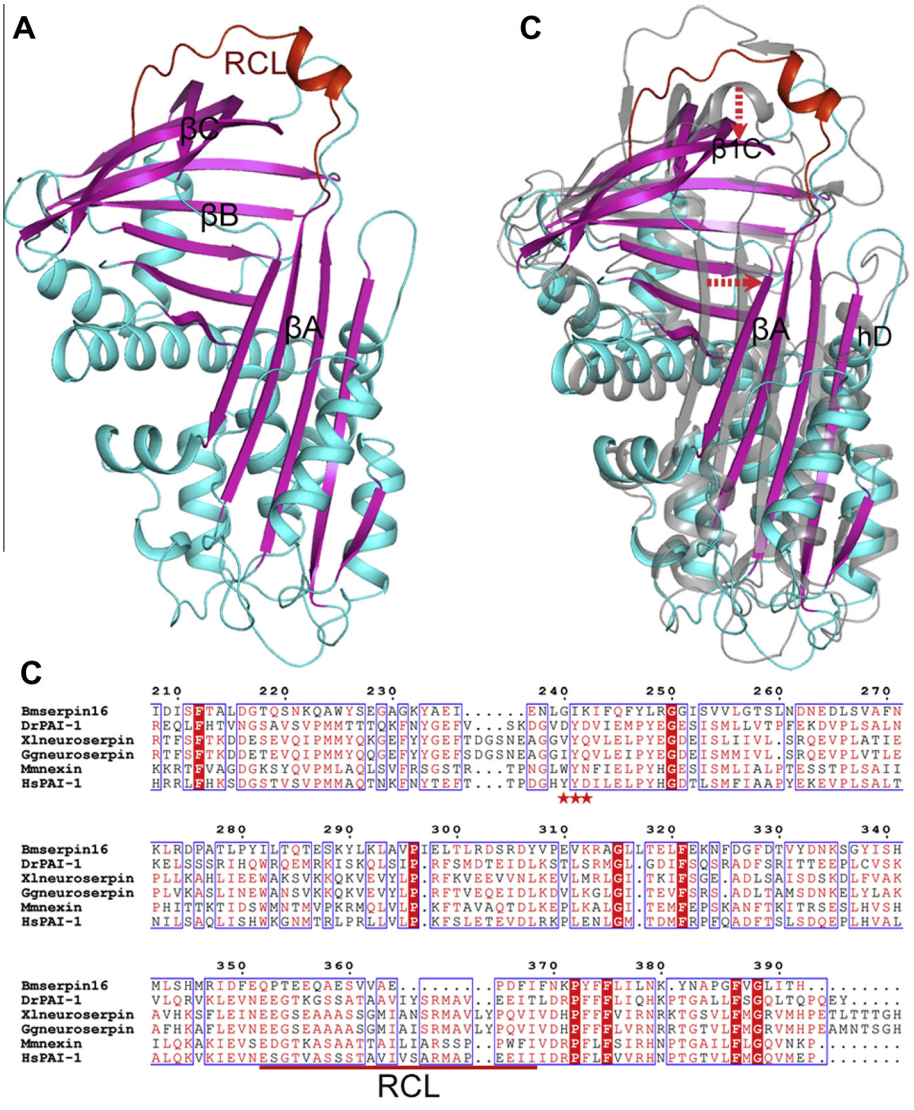

Fig. 2. Overall structure of serpin16. (A) Schematic representation of serpin16 fold. Cyan, helical subdomain; red, RCL; magenta, the three β-sheets. (B) Comparison of the overall structure between serpin16 and human plasminogen activator inhibitor-1 (PDB: 1DB2, gray). All figures were prepared using *PyMOL*. (C) Multiple sequence alignments of *Bombyx mori* serpin16 (NP_001139708.1); DrPAI-1, *Danio rerio* plasminogen activator inhibitor-1 (XP_009301297.1); Xlneuroserpin, *Xenopus laevis* neuroserpin (NP_001089150.1); Ggneuroserpin, *Gallus gallus* neuroserpin (NP_001004411.1); *Ms*nexin, *Mus musculus* nexin (NP_033281.1) and *Hs*PAI-1, *Homo sapiens* plasminogen activator inhibitor-1 (NP_000593.1). The residues constituted the negatively charge path on the β-sheet B in *Hs*PAI-1 are marked with red stars. Alignments were performed with *ClustalW* [32] and *ESPript* [33]. (For interpretation of the references to colour in this figure legend, the reader is referred to the web version of this article.)

proteinases. The residual proteolytic activities of trypsin, chymotrypsin, elastase, subtilisin, and proteinase K each decreased by ~5–10%, implying that serpin16 has almost no inhibitory activity towards these serine proteinases. However, serpin16 showed inhibitory activity towards papain, as the proteolytic activity of papain was reduced by ~38% (Fig. 3A). Inhibition assay data showed that serpin16 could inhibit papain in a dose-dependent manner (Fig. S3A). Moreover, the mammalian lysosomal cysteine proteinase, cathepsin L, was also inactivated by serpin18 (Fig. 3A). These findings demonstrated that serpin16 might act as a type of cysteine proteinase inhibitor, instead of as a serine proteinase inhibitor.

Moreover, to explore whether the shortening of seven residues in the RCL makes serpin16 lose inhibitory activity towards serine proteinases compared to typical serpins, we added the seven residues (-AVIVSAR-, according the typical serpin *Hs*PAI-1) into the RCL of serpin16 (designated as "serpin16Plus") and measured its activity (Fig. 3B). However, the inhibitory activities towards the serine proteinases by "serpin16Plus" were not detected, similar to that of the wild-type serpin16. Meanwhile, the mutation retained the inhibitory activities towards cysteine proteinases (Fig. 3C). Both protein samples were quality controlled using circular dichroism spectroscopy, indicating that the extension by seven residues did not introduce significant changes into the protein structure (Fig. S3B). It is thus these findings suggested that the target specificity of serpin16 did not only depend on the RCL, although serpins do use the RCL to bait target proteases.

3.4. Structural basis for the target specificity of serpin16

A critical step in the covalent trapping of a proteinase by a serpin is the initial formation of a Michaelis complex [28]. For non-serpin inhibitors, this is the only step involved in inhibition [29]. Thus, the recognition and interactions between the proteinase and inhibitor within the Michaelis complex depend on the target specificity and stability of the complex. To explore the structural basis for the specific recognition of a cysteine proteinase by serpin16, we simulated a model of the serpin16–papain Michaelis complex using the program HADDOCK [25], based on our serpin16 model and a previously reported structure of papain (PDB: 1PPP). The complex was predicted to be restrained by interactions between the active site residues of serpin16 and papain, as defined by the program WHISCY [30]. Among the four output clusters that were generated, the cluster of lowest energy with 94 numbers satisfied the optimal interaction restraints. The overall backbone RMSD of 0.8 ± 0.4 Å for the 94 members indicated that the serpin16–papain model was somewhat reliable.

In our model of the complex, papain is situated above the serpin16 molecule, and the RCL of serpin16 acts as an "antenna" that docks at the substrate-binding cleft of papain (Fig. 4A). The interface buries an area of ~1280 Å^2 (626 Å^2 for serpin16, 655 Å^2 for papain) and contains six hydrogen bonds between serpin16 and papain (Fig. S3A). Additionally, several hydrophobic interactions act to further stabilize the interface (Gly23, Cys25, Tyr61, Gly65, Gly66, Tyr67, Trp69, and Val157 of papain; Ile208, Gly229, Tyr290, Ser360, Val361, Val362, and Ala363 of serpin16) (Fig. S3B). Thus, papain makes extensive interactions with the RCL and the surfaces of β-sheet B and C in serpin16. A similar binding pattern was also observed in the Michaelis complex formed by typical serpin and serine proteinase, such as the *Hs*PAI-1–uPA complex (uPA, urokinase-type plasminogen activator, a serine proteinase) [31]. However, a structural comparison showed that the proteinase-binding interface of serpin16 is substantially different from that of the typical serpin *Hs*PAI-1 (Fig. 4B2 and C2). In *Hs*PAI-1, the RCL is long enough to reach the bottom of the deep substrate-binding cleft of a serine proteinase, and the alkaline residue (P1′) of RCL can bind to the acidic region located at the cleft bottom of the proteinase (N1′) (Fig. 4C1 and C2). By contrast, the RCL of serpin16 is significantly shorter than that of a typical serpin and lacks the conserved alkaline residue; but it possesses an acidic residue (N1) that can bind to the alkaline region (P1) located at the bottom of papain (Fig. 4B1 and B2). Additionally, the surface of the *Hs*PAI-1 β-sheet B displays a highly negative electrostatic patch (N2′) to interact with a corresponding positively charged patch (P2′) on the serine proteinase exosites (Fig. 4C1 and C2), whereas the surface of the β-sheet B in serpin16 displays a relatively positive electrostatic potential (P2). Moreover, multiple alignments revealed that the residues constituted the negatively charge path

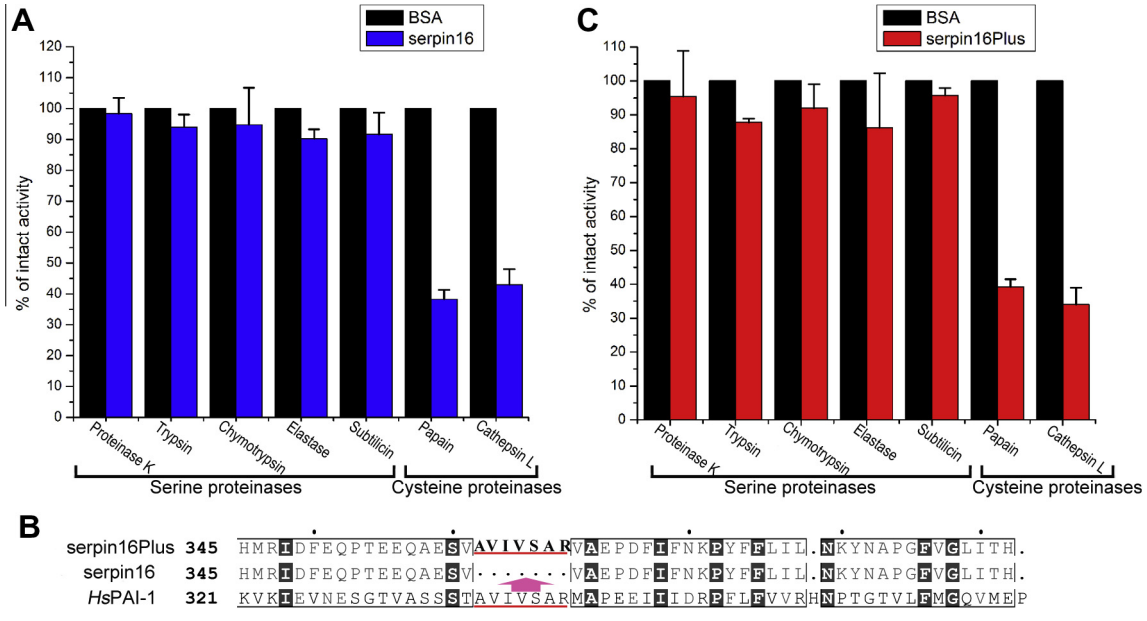

Fig. 3. The inhibitory activity of serpin16. (A) The bar graph diagrams of residual activities of proteinases incubated with serpin16 at molar ratios (inhibitor: proteinase) of 5. (B) Schematic diagram of the construction of the "serpin16Plus" mutation. (C) The bar graph diagrams of residual activities of proteinases incubated with "serpin16Plus".

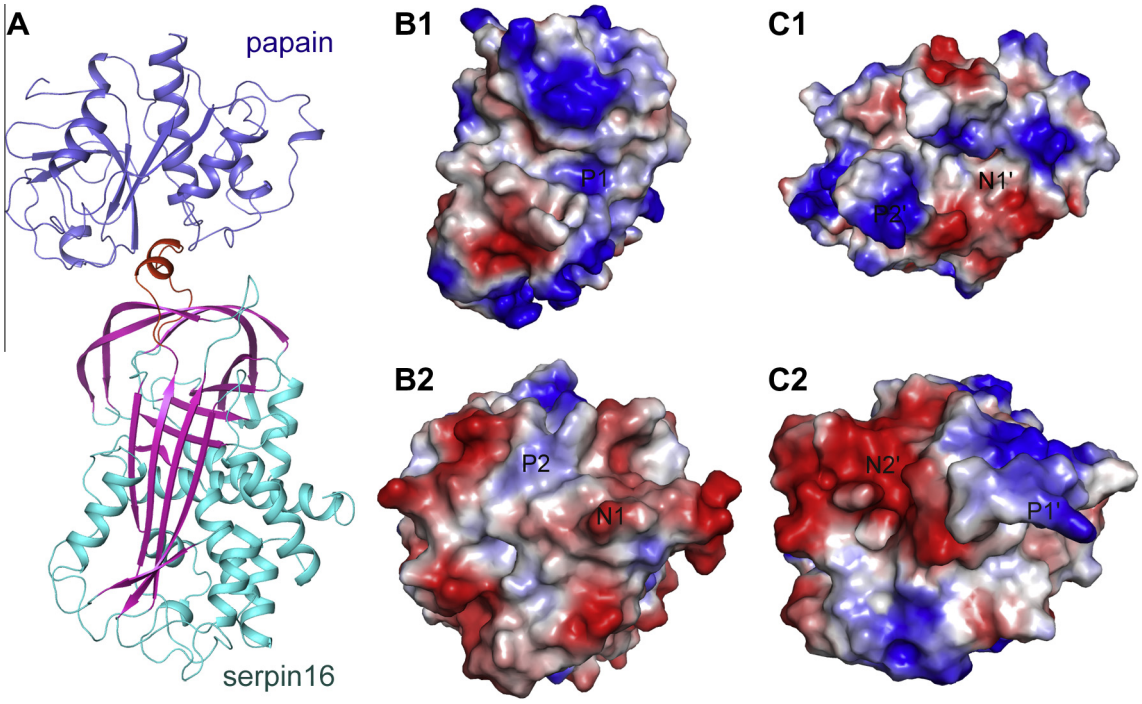

Fig. 4. Structural analysis of serpin16–papain Michaelis complex. (A) Overall structure of the Michaelis complex. Top, papain; bottom, serpin16. (B) Charge distribution on the binding-interface of (B1) papain and (B2) serpin16; P1, P2 and N1 represent the positively and negatively charged surfaces, respectively. (C) Charge distribution on the binding-interface of (C1) serine proteinase uPA and (C2) inhibitor *Hs*PAI-1; P1′, P2′ and N1′, N2′ represent two positively and two negatively charged surfaces, respectively.

(N2′) in *Hs*PAI-1 are highly conserved in the typical serpins (Fig. 2C). Thus, these structural features constitute the foundation of serpin16 specificity for a cysteine proteinase, but not a serine proteinase.

In summary, this study has identified a silk gland-specific inhibitor serpin16, which shows inhibitory activity towards cysteine proteinase. Moreover, a homology model of serpin16 and a docking model with its target proteinase were constructed. These structures provide the structural basis for understand the specificity of serpin16 for cysteine proteinase. However, more investigation are needed to elucidate the inhibitory mechanism and physiological role and of serpin16 in the silk gland.

Acknowledgments

We thank the staffs at Shanghai Synchrotron Radiation Facility for the data collection, and we are grateful to all the developers of CCP4 Suit, ESPript and PyMOL. This work was supported by the National Hi-Tech Research and Development Program of China (2011AA100306), the National Natural Science Foundation of China (31472154) and the China Postdoctoral Science Foundation (2014T70843 and 2013M542245).

Appendix A. Supplementary data

Supplementary data associated with this article can be found, in the online version, at http://dx.doi.org/10.1016/j.bbrc.2014.12.056.

References

[1] J. Travis, G.S. Salvesen, Human plasma proteinase inhibitors, Annu. Rev. Biochem. 52 (1983) 655–709.
[2] R.W. Carrell, P.A. Pemberton, D.R. Boswell, The serpins: evolution and adaptation in a family of protease inhibitors, Cold Spring Harb. Symp. Quant. Biol. 52 (1987) 527–535.
[3] J.A. Huntington, R.J. Read, R.W. Carrell, Structure of a serpin–protease complex shows inhibition by deformation, Nature 407 (2000) 923–926.
[4] P.G. Gettins, Keeping the serpin machine running smoothly, Genome Res. 10 (2000) 1833–1835.
[5] N.D. Rawlings, D.P. Tolle, A.J. Barrett, Evolutionary families of peptidase inhibitors, Biochem. J. 378 (2004) 705–716.
[6] A.M. Valeri, S.M. Wilson, R.D. Feinman, Reaction of antithrombin with proteases. Evidence for a specific reaction with papain, Biochim. Biophys. Acta 614 (1980) 526–533.
[7] M.A. Curtis, M. Macey, J.M. Slaney, G.L. Howells, Platelet activation by Protease-I of Porphyromonas-gingivalis W83, FEMS Microbiol. Lett. 110 (1993) 167–174.
[8] L.T. Hunt, M.O. Dayhoff, A surprising new protein superfamily containing ovalbumin, antithrombin-III, and alpha 1-proteinase inhibitor, Biochem. Biophys. Res. Commun. 95 (1980) 864–871.
[9] R.F. Doolittle, Angiotensinogen is related to the antitrypsin-antithrombin-ovalbumin family, Science 222 (1983) 417–419.
[10] I.L. Flink, T.J. Bailey, T.A. Gustafson, B.E. Markham, E. Morkin, Complete amino acid sequence of human thyroxine-binding globulin deduced from cloned DNA: close homology to the serine antiproteases, Proc. Natl. Acad. Sci. U.S.A. 83 (1986) 7708–7712.
[11] P.A. Pemberton, P.E. Stein, M.B. Pepys, J.M. Potter, R.W. Carrell, Hormone binding globulins undergo serpin conformational change in inflammation, Nature 336 (1988) 257–258.
[12] P.E. Stein, A.G.W. Leslie, J.T. Finch, W.G. Turnell, P.J. Mclaughlin, R.W. Carrell, Crystal-structure of ovalbumin as a model for the reactive center of serpins, Nature 347 (1990) 99–102.
[13] T. Sasaki, K. Kobayashi, Isolation of two novel proteinase inhibitors from hemolymph of silkworm larva, *Bombyx mori*. Comparison with human serum proteinase inhibitors, J. Biochem. 95 (1984) 1009–1017.
[14] M.R. Kanost, Isolation and characterization of four serine proteinase inhibitors (serpins) from hemolymph of *Manduca sexta*, Insect Biochem. 20 (1990) 141–147.
[15] Y. Wang, H. Jiang, Purification and characterization of *Manduca sexta* serpin-6: a serine proteinase inhibitor that selectively inhibits prophenoloxidase-activating proteinase-3, Insect Biochem. Mol. Biol. 34 (2004) 387–395.
[16] K.R. Stark, A.A. James, Isolation and characterization of the gene encoding a novel factor Xa-directed anticoagulant from the yellow fever mosquito *Aedes aegypti*, J. Biol. Chem. 273 (1998) 20802–20809.
[17] Z. Zou, Z. Picheng, H. Weng, K. Mita, H. Jiang, A comparative analysis of serpin genes in the silkworm genome, Genomics 93 (2009) 367–375.
[18] H. Takagi, H. Narumi, K. Nakamura, T. Sasaki, Amino acid sequence of silkworm (*Bombyx mori*) hemolymph antitrypsin deduced from its cDNA nucleotide sequence: confirmation of its homology with serpins, J. Biochem. 108 (1990) 372–378.
[19] T. Sasaki, K. Kobayashi, T. Ozeki, Interaction of silkworm larval hemolymph antitrypsin and bovine trypsin, J. Biochem. 102 (1987) 433–441.

[20] H. Narumi, T. Hishida, T. Sasaki, D.F. Feng, R.F. Doolittle, Molecular cloning of silkworm (*Bombyx mori*) antichymotrypsin. A new member of the serpin superfamily of proteins from insects, Eur. J. Biochem. 214 (1993) 181–187.
[21] Y. Hou, Q. Xia, P. Zhao, Y. Zou, H. Liu, J. Guan, J. Gong, Z. Xiang, Studies on middle and posterior silk glands of silkworm (*Bombyx mori*) using two-dimensional electrophoresis and mass spectrometry, Insect Biochem. Mol. Biol. 37 (2007) 486–496.
[22] F. Kiefer, K. Arnold, M. Kunzli, L. Bordoli, T. Schwede, The SWISS-MODEL repository and associated resources, Nucleic Acids Res. 37 (2009) D387–D392.
[23] K. Arnold, L. Bordoli, J. Kopp, T. Schwede, The SWISS-MODEL workspace: a web-based environment for protein structure homology modelling, Bioinformatics 22 (2006) 195–201.
[24] T. Schwede, J. Kopp, N. Guex, M.C. Peitsch, SWISS-MODEL: an automated protein homology-modeling server, Nucleic Acids Res. 31 (2003) 3381–3385.
[25] S.J. de Vries, M. van Dijk, A.M. Bonvin, The HADDOCK web server for data-driven biomolecular docking, Nat. Protoc. 5 (2010) 883–897.
[26] M.Z. Djie, B.F. Le Bonniec, P.C. Hopkins, K. Hipler, S.R. Stone, Role of the P2 residue in determining the specificity of serpins, Biochemistry 35 (1996) 11461–11469.
[27] A.W. Zhou, R.W. Carrell, J.A. Huntington, The serpin inhibitory mechanism is critically dependent on the length of the reactive center loop, J. Biol. Chem. 276 (2001) 27541–27547.
[28] S. Ye, A.L. Cech, R. Belmares, R.C. Bergstrom, Y. Tong, D.R. Corey, M.R. Kanost, E.J. Goldsmith, The structure of a Michaelis serpin–protease complex, Nat. Struct. Biol. 8 (2001) 979–983.
[29] P.G. Gettins, Serpin structure, mechanism, and function, Chem. Rev. 102 (2002) 4751–4804.
[30] S.J. de Vries, A.D.J. van Dijk, A.M.J.J. Bonvin, WHISCY: what information does surface conservation yield? Application to data-driven docking, Proteins-Struct. Funct. Bioinform. 63 (2006) 479–489.
[31] Z. Lin, L. Jiang, C. Yuan, J.K. Jensen, X. Zhang, Z. Luo, B.C. Furie, B. Furie, P.A. Andreasen, M. Huang, Structural basis for recognition of urokinase-type plasminogen activator by plasminogen activator inhibitor-1, J. Biol. Chem. 286 (2011) 7027–7032.
[32] M.A. Larkin, G. Blackshields, N.P. Brown, R. Chenna, P.A. McGettigan, H. McWilliam, F. Valentin, I.M. Wallace, A. Wilm, R. Lopez, J.D. Thompson, T.J. Gibson, D.G. Higgins, Clustal W and Clustal X version 2.0, Bioinformatics 23 (2007) 2947–2948.
[33] P. Gouet, X. Robert, E. Courcelle, ESPript/ENDscript: extracting and rendering sequence and 3D information from atomic structures of proteins, Nucleic Acids Res. 31 (2003) 3320–3323.